

## ANALYTICAL DESCRIPTION OF THE INFLUENCE OF THE QUANTUM SUSCEPTANCE ON THE PERFORMANCE OF SIS MIXERS

Pascal FEBVRE

DEMIRM - Observatoire de PARIS-MEUDON  
5, place Jules JANSSEN - 92195 Meudon Cedex - FRANCE

### ABSTRACT

A new analytical formalism has been used to describe the contours of constant mixer output conductance and constant available conversion gain in the source admittance plane. This analysis is valid for Double Side-Band mixers in the three-frequency approximation using the low IF limit. The influence of the small-signal admittance matrix reactive terms and of the quantum susceptance is studied in the particular case of SIS mixers. The three different regimes of operation of an SIS mixer are described. The regions in the source admittance plane for optimum receiver performance are discussed. It is shown that the optimum  $\omega R_N C$  product is dependent on the losses of the microwave environment of the mixer. This analytical and graphical formalism is shown to be an efficient tool to understand the behaviour of mixers and ease their design.

### I. INTRODUCTION

The quantum theory of mixing developed by Tucker [1, 2] has been widely used to predict the performance of SIS mixers using either the three or five-frequency approximations. Good agreements between theory and experiments have been found up to 100 GHz [3-5]. But the complexity of the quantum theory of mixing associated with the large number of free parameters (Local Oscillator power, DC bias voltage, IF and RF port admittances, frequency of operation, quality of the I-V curve) makes difficult the prediction of performances in the general case. Computer simulations are generally used to find the parameters of SIS mixers which give optimum performance [6-9] or to compare a posteriori theoretical predictions with experimental results [3-5, 10-11]. Some attempts to describe analytically the behaviour of SIS mixers have been made in the low LO limit [12-14], but the quantum reactive terms of the small-signal matrix are sometimes neglected to simplify the analysis since it has been argued that they have little

effect on the performance of SIS mixers [13,15]. But this last approximation has been a controversial subject [16, 17].

One presents here a different analytical formalism which allows to understand how the performance of an SIS mixer is affected by several free parameters accessible to the experimentalists. The quantum reactive terms of the small-signal matrix are taken into account and their influence is studied quantitatively. In this treatment the interferences from Josephson effects are not considered and the analysis is limited to Double Side-Band SIS mixers in the low IF limit using the three-frequency approximation. These assumptions are commonly used since they correspond to most of the practical mixers in operation and under development up to 700 GHz. Moreover, most of the current SIS receiver developments above 300 GHz use tuning circuits to resonate the SIS intrinsic parasitic capacitance at the operating frequency [18-21]. The three-frequency approximation is then a good assumption since the harmonics of signal, image and Local Oscillator (LO) frequencies are shunted by the SIS specific capacitance which is not resonated any more by the tuning circuit. Besides the SIS mixer is operated as a Double Side-Band (DSB) mixer since the Intermediate Frequency is lower than the instantaneous RF bandwidth at the resonance frequency of the SIS junction specific capacitance with the tuning circuit.

With these assumptions the IF output impedance of the mixer as well as its conversion gain can be calculated analytically [2]. These quantities are expressed in this paper in a more convenient form to be easily treated analytically and graphically. One shows that such an analytical investigation in the general case is of great help to get an intuitive understanding of the behaviour of SIS mixers, to predict their optimum performance and to ease the design of practical receivers.

In this treatment the source and load admittances of the environment are not fixed but are free parameters in order to allow their determination for optimum performance. It is then possible to determine the contours of constant IF output admittance and constant available conversion gain in the source admittance plane. The regions of infinite available conversion gain and negative output differential resistance will be treated as particular cases of this analysis. A close analysis has been performed by Pan & Kerr [22] to determine analytically the regions of infinite available gain and negative output differential resistance in the same plane for Double Side-Band mixers. They also performed the calculations of the contours of constant conversion loss and the expression of the IF output admittance for Single Side-Band mixers. This last case will not be treated in this work.

The analytical expression of the IF conductance is presented and the corresponding graphical representation is described in part II. The ranges of LO powers and bias voltages for which the quantum reactive terms are necessary to correctly predict the mixer performance are determined in Part III for different LO frequencies. Part IV performs the analysis to determine the contours of constant mixer available conversion gain. Part V discusses the case of the optimum  $\omega R_N C$  product and finally the conclusion will be drawn in part VI.

## II. CONTOURS OF CONSTANT IF CONDUCTANCE IN THE $(G_S, B_S)$ PLANE

A mixer consists of a Local Oscillator at frequency  $\omega_{LO}$  applied on a non-linear device which is mixed with the sideband frequencies  $\omega_m = m \omega + \omega_0$ ,  $m = -1, 0, 1$  in the three-port approximation. Each sideband is assumed to be terminated by  $Y_i$  which is the admittance of the external microwave environment of the mixing device at port  $i$ . With the assumption of a Double Side-Band mixer with the low IF limit, one has the same admittance  $Y_S (= G_S + j B_S) = Y_1 = Y_{-1}^* = Y_{LO}$  at the signal, image and LO frequencies. These last three frequencies will be called RF frequencies in the following. The admittance of the environment at the Intermediate Frequency (IF) is noted  $Y_L = Y_0$ . Its real part is noted  $G_L$ .

The small-signal currents and voltages at each sideband are related by the small-signal admittance matrix terms which are written  $Y_{ij} = G_{ij} + j B_{ij}$  where  $i, j = -1, 0, 1$  in the three-port approximation. The values of  $B_{ij}$  are called the quantum reactive terms of the small-signal admittance matrix. The values of  $G_{ij}$  and  $B_{ij}$  have been given for SIS mixers in a convenient way in [2] with expressions (4.72) and (4.73). The augmented matrix  $\|Y'\|$  is defined by the terms  $Y'_{ij} = Y_{ij} + Y_i \delta_{ij}$ . Using some basic principles of frequency conversion the mixer IF admittance as well as the conversion gain can be estimated by inverting the augmented matrix [1, 2, 23]. One obtains:  $\|Z\| = \|Y'\|^{-1}$ . The IF impedance can be expressed as [2, 23]:

$$Y_{IF} = \frac{1}{(Z_{00})_{Y_L=0}} \quad (2.1)$$

In the case of a Double Side-Band Mixer, this admittance is real, it will be noted  $G_{IF}$  in the following. One sees from equation (2.1) and from the formalism of the augmented matrix that  $G_{IF}$  is a function of the values of  $Y_{ij}$  and  $Y_S$  only. This conductance is also the slope of the pumped I-V curve [2]. It can be expressed under the form:

$$G_{IF} = G_{00} - 2 G_{01} \frac{g_1^- G_{10} + b_1^- B_{10}}{g_1^- g_1^+ + b_1^- b_1^+} \quad (2.2)$$

where:

$$g_1^+ = G_s + G_{11} + G_{1-1} \quad \text{and} \quad g_1^- = G_s + G_{11} - G_{1-1} \quad (2.3)$$

$$b_1^+ = B_s + B_{11} + B_{1-1} \quad \text{and} \quad b_1^- = B_s + B_{11} - B_{1-1}$$

It can be easily shown that expressions (2.2) with (2.3) are identical to the expressions (4.77) with (4.75) given by Tucker and Feldman in Ref. [2].

From this simple analytical formulas, it is straightforward to show that the contour of constant IF conductance  $G_{IF}$  in the source admittance plane ( $G_s, B_s$ ) is a circle of center  $(X_G, Y_B)$  and radius  $R_0$  with:

$$X_G = \frac{G_{01} G_{10}}{G_{00} - G_{IF}} - G_{11} \quad (2.4)$$

$$Y_B = \frac{G_{01} B_{10}}{G_{00} - G_{IF}} - B_{11} \quad (2.5)$$

$$R_0 = \sqrt{R_G^2 + R_B^2} \quad (2.6)$$

$$R_G = \frac{G_{01} G_{10}}{G_{00} - G_{IF}} - G_{1-1} \quad (2.7)$$

$$R_B = \frac{G_{01} B_{10}}{G_{00} - G_{IF}} - B_{1-1} \quad (2.8)$$

It is important to notice that this description is not specific to SIS mixers but **it is valid for all Double Side-Band mixers using the three-frequency approximation in the low IF limit.**

The regions in the source admittance plane which give negative IF output conductance  $G_{IF}$  are also associated with infinite available conversion gain (see paragraph IV) and the above expressions (2.4) to (2.8) reduce to the expressions given in [22] if one takes  $G_L = -G_{IF}$ . In the present case the IF output admittance  $Y_L$  is not fixed and, as a consequence, though the available conversion gain is infinite, the coupled gain can vary depending on the value of  $Y_L$ .

This description in terms of contours in the  $(G_s, B_s)$  plane is valid for any set of  $Y_{ij}$ . The terms  $Y_{ij}$  of the small-signal matrix vary of course as a function of the shape of

the I-V curve, the RF frequencies, the LO power and the DC bias voltage. One will examine the influence of these parameters later.

Also, the radius of the circles is the square root of the sum of two terms. If the reactive terms of the small-signal admittance matrix are neglected, one clearly sees that the radius is smaller. This remark will be of particular importance for the following.

Figure 1 shows the geometrical construction of these circles in the  $(G_s, B_s)$  plane.

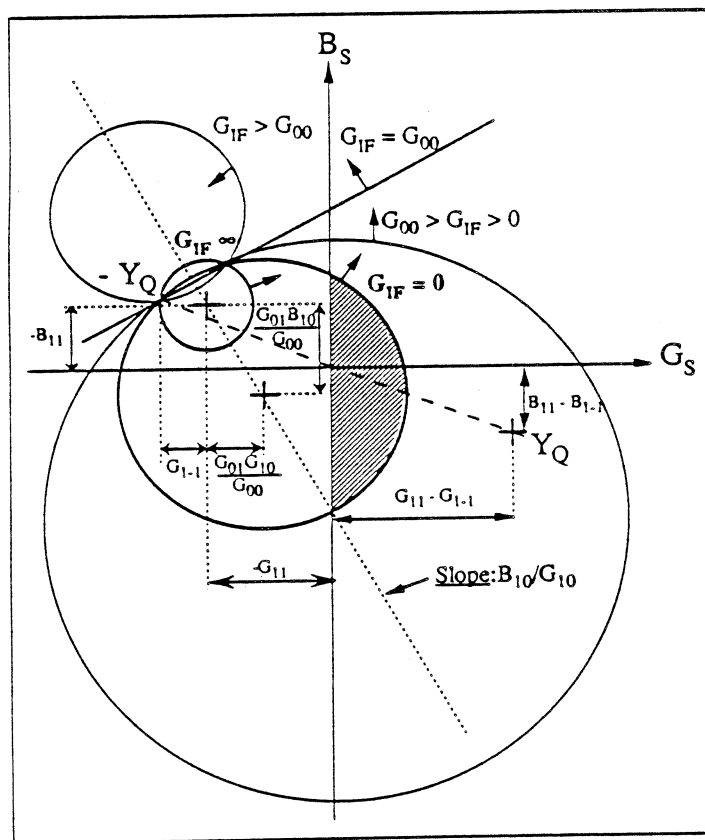


Figure 1: Contours of constant mixer IF output conductance  $G_{IF}$ . The hatched region corresponds to negative output conductance and infinite available gain.  $Y_Q$  is the large-signal admittance of the mixer at the LO frequency.

To understand this figure one can notice a few interesting features of these circles according to equations (2.4) to (2.8).

First, when the IF conductance varies, the centers of the circles in the  $(G_s, B_s)$  plane are located on a line whose slope is constant and given by  $B_{10}/G_{10}$ .

Second, the contour for  $G_{IF} = G_{00}$  is a line perpendicular to the line on which the centers of the circles are located. It corresponds to a circle of infinite radius.

At last, all these circles cross two particular points located on the  $G_{IF} = G_{00}$  line . One of these points is located at the admittance  $-Y_Q$  where  $Y_Q$  is the large-signal admittance of the mixer which is also called the quantum admittance. The real part of  $Y_Q$  is called the quantum conductance and named  $G_Q$ . The imaginary part is the quantum susceptance and called  $B_Q$ . They can be expressed as a function of some terms of the small-signal admittance matrix [23] according to the relations (2.9) and (2.10):

$$G_Q = G_{11} - G_{1-1} \quad (2.9)$$

$$B_Q = B_{11} - B_{1-1} \quad (2.10)$$

The zero IF output conductance circle, which is also a circle of infinite available gain has a particular importance: the region in the source admittance plane having a physical meaning and for which  $G_{IF}$  is negative is comprised inside this circle and in the half-plane corresponding to  $G_s > 0$  as it has been also noticed in Ref. [22]. It corresponds to the hatched region of figure 1. This circle is the border between two dual regions in the  $G_s > 0$  half-plane. Indeed, outside the hatched region the maximum coupled conversion gain is the available non-infinite conversion gain. Any source admittance in this region corresponds to a given positive IF output conductance of the mixer - i.e. to a given positive slope of the DC pumped I-V curve- and is located on one contour of constant IF mixer conductance  $G_{IF}$ . In this region the IF load conductance  $G_L$  must be equal to  $G_{IF}$  to reach the available conversion gain. Let us call these values  $G_{L,pos}$  and  $G_{avail,pos}$ .

But it is possible to find an other (dual) source admittance inside the hatched region (see figure 1) which gives **the same coupled conversion gain  $G_{avail,pos}$  with the same load admittance  $G_{L,pos}$** . Indeed, once  $G_{L,pos}$  is fixed, there is a source admittance in the hatched region of negative output differential resistance  $G_{IF}$  which gives the right output coupling  $\gamma$  with  $G_{L,pos}$  where  $\gamma$  is expressed under the form:

$$\gamma = \frac{4 G_{IF} G_{L,pos}}{|G_{IF} + G_{L,pos}|^2} \quad (2.11)$$

to provide a coupled gain equal to  $G_{avail,pos}$  since the available conversion gain is infinite (and corresponds to  $G_{IF} = -G_{L,pos} < 0$ ). The only difference in terms of mixer performance comes from the mixer noise which has no reason to be the same for these two different source admittances. Also, the hatched region corresponds to negative differential resistance in the I-V curve which is associated with possible oscillations and instabilities [3] and is not desirable for stable operation of a practical receiver. Then, two different modes of operation can be distinguished: one is unstable and corresponds to non

desirable conditions of operation of the receiver, the other one, corresponding to a positive differential resistance of the pumped I-V curve is more likely to be obtained in practical experiments and can be associated to high but not infinite available conversion gain.

It is interesting to mention that the condition given in Ref. [15] and expressed as:

$$G_S + G'_S = 0 \quad (2.12)$$

which allows to determine two different modes of operation does exactly correspond to the source conductances within the hatched region of figure 1 when the quantum reactive terms are neglected. Indeed the expression of  $G'_S$  given in Ref. [15] is  $-(X_G + R_G)$  with expressions (2.4) and (2.7) and corresponds to the maximum source conductance of the circles of negative  $G_{IF}$ . Then the two different modes of operation described in Ref. 15 when the quantum reactive terms are neglected correspond to the two different regions (hatched and not hatched) shown in figure 1.

### III. INFLUENCE OF THE QUANTUM REACTIVE TERMS

Once the analytical description of the contours of constant IF output conductance  $G_{IF}$  of the mixer is performed, it is straightforward to study the influence of the quantum reactive terms. To do that, one will first neglect them. In that case the circle of zero  $G_{IF}$  is smaller as is shown in figure 2 which is the same figure as figure 1 where all the  $B_{ij}$ 's have been set to zero. By comparing these two figures, one clearly sees that the regions in the source admittance plane ( $G_S$ ,  $B_S$ ) for which there is a possibility of infinite available gain and negative differential output conductance are shrunk when quantum reactive terms are neglected. It means that the reactive terms and, as a consequence, the quantum susceptance obtained with (2.10), increase the range of possibilities for infinite available gain. This corroborates some conclusions of Ref. [16-17] and makes the case very general. Also one can argue that the quantum susceptance is not directly responsible for that effect but is more a consequence of the presence of quantum reactances in the small-signal admittance matrix. Indeed, one sees in figure 1 that the quantity  $(G_{01} B_{10})/G_{00}$  is of particular importance to account for the smaller radius of the circle of zero  $G_{IF}$ .

One will now choose the criterium of the possibility of infinite available gain to determine the influence of the reactive terms. As any criterium, it is questionable but it allows to determine the ranges of parameters for which a typical quantum effect of a

mixer like negative differential output conductance can occur. A good other criterium could have been the possibility to get conversion gain versus conversion loss.

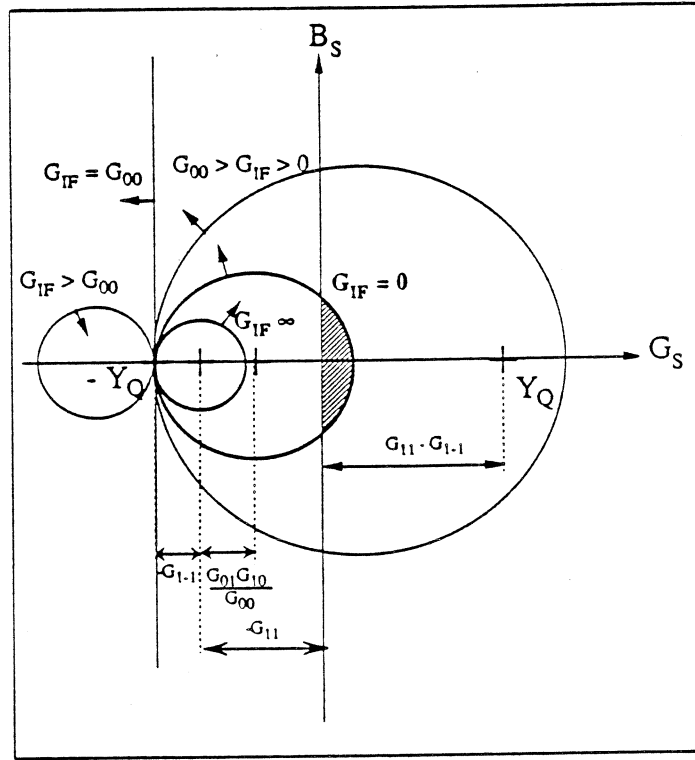


Figure 2: Contours of constant mixer IF output conductance  $G_{IF}$ . In this figure the quantum reactive terms  $B_{ij}$  have been set to zero. The hatched region corresponds to negative output conductance and infinite available gain, it is smaller than in figure 1.

Though the analysis of the ranges of parameters for which infinite available gain is possible does not allow to predict the parameters for optimum performance, it is a useful tool to target the regions in the source admittance plane where good mixer performance is possible and then to ease their design.

### III.1 Quantum reactive terms neglected

When the reactive terms are neglected it is possible to have infinite available gain if part of the  $G_{IF} = 0$  circle crosses the half-plane  $G_s > 0$  in the source admittance plane. Analytically it corresponds to the relation:

$$(X_G + |R_G|)_{G_{IF}=0} \geq 0 \tag{3.1}$$



which can be rewritten:

$$\frac{G_{01} G_{10}}{G_{00}} \geq \frac{G_{11} + G_{1-1}}{2} \quad (3.2)$$

If one calls:

$$\eta = \frac{2 G_{01} G_{10}}{G_{00} (G_{11} + G_{1-1})} \quad (3.3)$$

the inequality (3.2), which is the criterium of possibility of infinite available gain when quantum reactive terms are neglected, can be expressed under the form

$$\eta \geq 1 \quad (3.4)$$

This is the relation given by Tucker & Feldman in Ref. [2] to predict the same possibility of unlimited gain and negative differential resistance.

### III.2 Quantum reactive terms taken into account

In this case, the inequality (3.1) must be replaced by:

$$(X_G + R_0)_{G_{IF}=0} \geq 0 \quad (3.5)$$

where the radius is now a function of conductive and reactive terms. Inequality (3.5) becomes:

$$\frac{G_{01} G_{10}}{G_{00}} \geq \frac{G_{11} + r G_{1-1}}{1 + r} \quad \text{or} \quad \frac{G_{01} G_{10}}{G_{00}} \leq \frac{G_{11} - r G_{1-1}}{1 - r} \quad (3.6)$$

with:

$$r = \sqrt{1 + \frac{R_B^2}{R_G^2}} \quad (3.7)$$

The two inequalities of (3.6) cannot be true at the same time, they represent the general condition to obtain infinite available conversion gain, they reduce to (3.2) or (3.4) if one neglects the reactive terms.

### III.3 Description of the different regimes of operation of SIS mixers

The influence of the quantum reactive terms can be examined by finding the ranges of parameters for which inequalities (3.2) and (3.6) are true or false. These parameters are the I-V curve quality, RF frequencies, DC bias voltage  $V_0$  and RF voltage  $V_{LO}$  through the parameter  $\alpha = (e V_{LO}) / (h \nu)$ . They influence the mode of operation of the mixer through the terms  $G_{ij}$  and  $B_{ij}$ .

It is straightforward to see using (3.2) and (3.6) that if (3.6) is false then (3.2) is also false. Practically it means that if it is not possible to predict infinite available conversion gain by including the reactive terms in the calculation then, a fortiori, there is no possibility to predict infinite gain if these terms are neglected. Then three different cases remains, they correspond to three different regimes of operation of the mixer.

1) (3.2) and (3.6) are false: it means that there is no possibility of infinite available gain. One will call this regime of operation "classical regime" since the mixer basically behaves like a classical mixer though, in that case, the criterium of unity conversion gain would have been better than this criterium of infinite available gain since there is still some possibility for absolute conversion gain. This case is illustrated in figure 3-a. The dashed circle is the zero IF conductance contour when reactive terms are neglected and the solid circle represents the contour for the same zero  $G_{IF}$  with reactive terms included in the calculation. Since none of these circles crosses the half-plane  $G_S > 0$  then there is no possibility for infinite available gain.

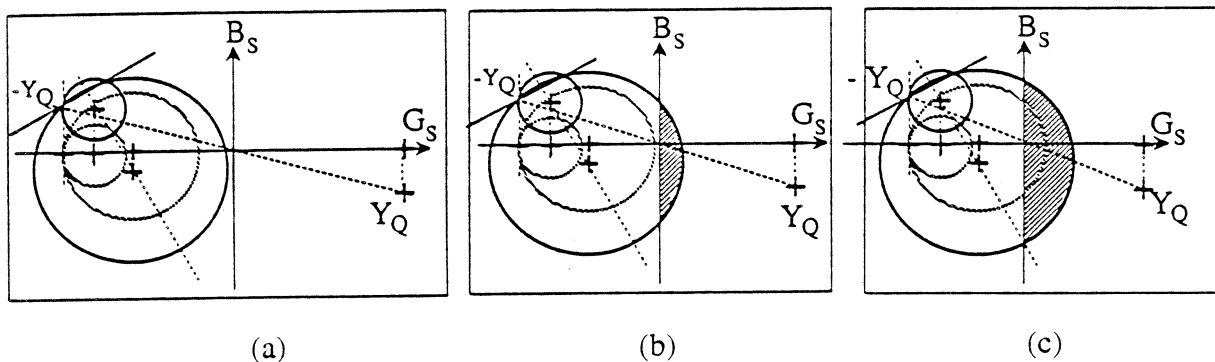


Figure 3: Contours of zero mixer IF output conductance  $G_{IF}$  with reactive terms included (solid circle) and neglected (dashed circle). Figure 3-a corresponds to the classical regime since there is no possibility of negative resistance on the half-plane  $G_S > 0$ . Figure 3-b shows the quantum reactive regime. At last figure 3-c displays the case of pure quantum regime where one can clearly see that the reactive terms increase the size of the hatched region for which infinite available gain is possible.

2) (3.2) is false and (3.6) is true: in that case it is not possible to predict infinite available gain if one neglects the quantum reactive terms but there are some source admittances for which infinite available gain is possible, see figure 3-b. It means that the quantum reactive terms are essential to account for unlimited gain and negative output differential resistance as it has been noticed in Ref. [16, 17]. One will call this mode of

operation "quantum reactive regime" since the reactive terms are necessary to provide infinite available gain. Infinite available gain occurs in the hatched region of figure 3-b.

3) (3.2) and (3.6) are true: infinite available gain is predicted even if the quantum reactive terms are neglected which corresponds to a "quantum conductive regime" since the conductive terms are sufficient to explain unlimited gain. These cases have been theoretically considered by Feldman in Ref. [13]. But the reactive terms widen the region in the source admittance plane for which infinite gain is possible. It means that both conductive and reactive terms influence the mixer behaviour. This regime is called "pure quantum regime". One can see in figure 3-c how the reactive terms increase the size of the hatched region of unlimited gain.

It is now possible to determine in which regime the mixer operates as a function of the parameters which control the values of the small-signal admittance matrix terms.

One will examine here only the influence of the RF frequency,  $\alpha$  and  $V_0$  for a given I-V curve shown in figure 4-d. Three graphs showing the different regimes of operation are shown in figures 4-a, 4-b and 4-c at three frequencies normalized to the gap frequency which are respectively 0.15, 0.84 and 1.09. They correspond to 100 GHz, 540 GHz and 700 GHz respectively for Nb/AlOx/Nb junctions. The abscissa axis shows the DC bias voltage  $V_0$  normalized to the gap voltage of the junction and the ordinate axis displays the RF voltage through the parameter  $\alpha$  in figures 4-a, 4-b and 4-c. The corresponding calculated pumped I-V curves are shown in figures 4-d, 4-e and 4-f.

The white regions of figures 4-a, 4-b and 4-c correspond to the classical regime of the SIS mixer, the hatched regions show the quantum reactive regime and the darken regions correspond to the pure quantum regime for which the quantum reactive terms are not necessary to predict unlimited gain.

One can first notice that it is possible to predict most of the regions of infinite available gain by neglecting the reactive terms at 100 GHz since the darken regions fill most of the hatched regions on the first two photon steps. It is not the case any more at 540 and 700 GHz where most of the  $V_0$  and  $\alpha$  ranges for which infinite gain is possible correspond to the quantum reactive regime.

An interesting feature appears at 540 GHz for a reduced voltage of about 0.7 indicated in figures 4-b and 4-e by a dashed line. One can see that there is an inflection point in the pumped I-V curve of figure 4-e which can be understood as the overlap of the second-order photon step from the negative voltage part of the I-V curve [20, 24]. In the following one will call overlap voltage the voltage at the inflection point in the pumped I-V curve. For voltages higher than this overlap voltage one sees that the range of values

of  $\alpha$  for which unlimited gain is possible is larger than below the overlap voltage. It means that good performance is still possible for lower voltages but for a limited range of values of  $\alpha$  corresponding to lower LO powers. As a consequence a mixer operating with LO powers corresponding to values of  $\alpha$  around 1.2 in this particular case will perform better for voltages higher than the overlap voltage [20,24]. Such an inflection point has also been observed at 540 GHz in figure 9 of Ref. [21] and was associated to a dip in the IF power versus DC voltage curve.

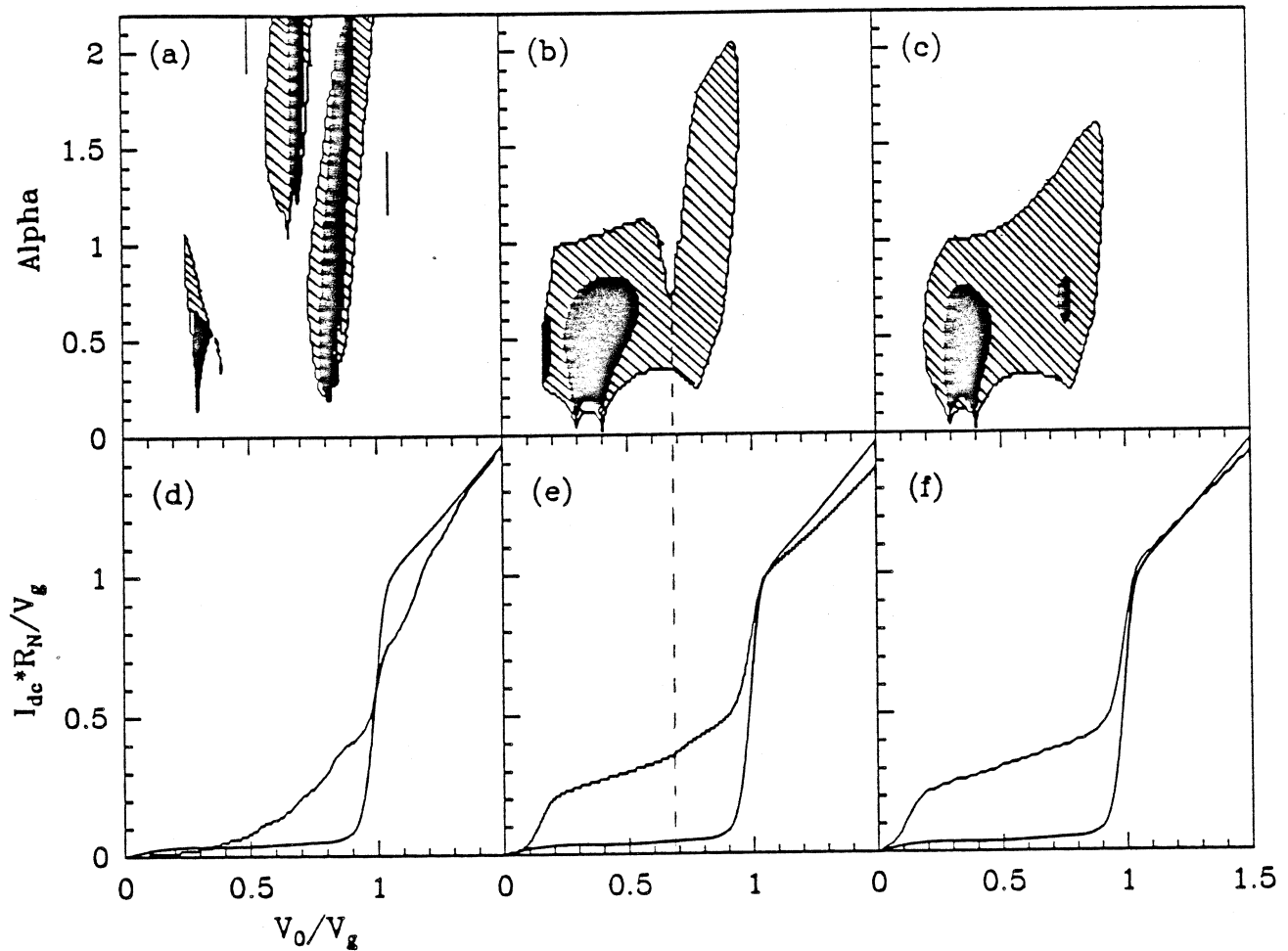


Figure 4: Regions of classical regime (white regions), quantum reactive regime (hatched regions) and pure quantum regime (darken regions) in the  $(V_0, \alpha)$  plane for three different frequencies: 100 GHz in figure 4-a, 540 GHz in figure 4-b, 700 GHz in figure 4-c. The corresponding calculated pumped I-V curves are shown respectively in figures 4-d, 4-e and 4-f.

Remark: Some darken and hatched regions appear at 100 GHz for reduced voltages close to 0.2-0.3, the physical reason for that is not known but may be due to computational errors caused by a too strong smoothing of the unpumped I-V curve at these voltages.

#### IV. CONTOURS OF CONSTANT AVAILABLE CONVERSION GAIN

The knowledge of the contours of constant conversion gain are of particular importance to study the behaviour of a mixer. Some analytical formulas have been derived for Single Side-Band mixers [22]. One presents here analytical formulas for Double Side-Band mixers. In the general case the contours of constant conversion gain do not have simple geometrical expressions. But it is possible to make some additional assumptions which are true in most of cases. These assumptions are the following:

$$|G_{1-1}| \ll G_{11} \quad (4.1)$$

$$|B_{1-1}| \ll |B_s + B_{11}| \quad (4.2)$$

(4.1) is true most of time and (4.2) means that the contours of constant conversion gain slightly deviates from the analytical form given below inside a strip of susceptances  $B_s$  centered at the susceptance  $-B_{11}$  and of width  $2|B_{1-1}|$  in the source admittance plane.

The conversion gain can be expressed under the form:

$$G_m = \gamma \frac{G_s G_{01}^2 \left( (g_i^-)^2 + (b_i^-)^2 \right)}{\left( g_i^- g_i^+ + b_i^- b_i^+ \right)^2} \frac{1}{G_{FI}} = \gamma G_m^0 \quad (4.3)$$

where the output coupling factor  $\gamma$  is defined by (2.11). The available conversion gain is  $G_m^0 = (L_m^0)^{-1}$ . It is possible to show that, according to the assumptions (4.1) and (4.2), the contours of constant available gain are circles of center  $(x_g, y_b)$  and radius  $r_0$  with:

$$x_g = \frac{G_{01}}{G_{00}} \left( G_{10} + \frac{G_{01}}{2} L_m^0 \right) - G_{11} \quad (4.4)$$

$$y_b = \frac{G_{01} B_{10}}{G_{00}} - B_{11} \quad (4.5)$$

$$r_0 = \sqrt{r_g^2 + r_b^2} \quad (4.6)$$

$$r_{sg}^2 = \left(\frac{G_{01}}{G_{00}}\right)^2 \left[ \left(G_{10} + \frac{G_{01}}{2} L_m^0\right)^2 - L_m^0 G_{00} G_{11} \right] \quad (4.7)$$

$$r_b = \frac{G_{01} B_{10}}{G_{00}} \quad (4.8)$$

When there is a possibility of infinite available gain these circles always cross the same two points on the  $B_S$  axis which are located on the contour of zero IF conductance as is shown in figure 5. One can notice that the circle of infinite available gain ( $L_m^0 = 0$ ) is also the circle of  $G_{IF} = 0$ . When  $L_m^0 < 0$  the available gain is still infinite through the parameter  $\gamma$  which can be infinite if the IF output match is such that  $G_L = -G_{IF}$ .

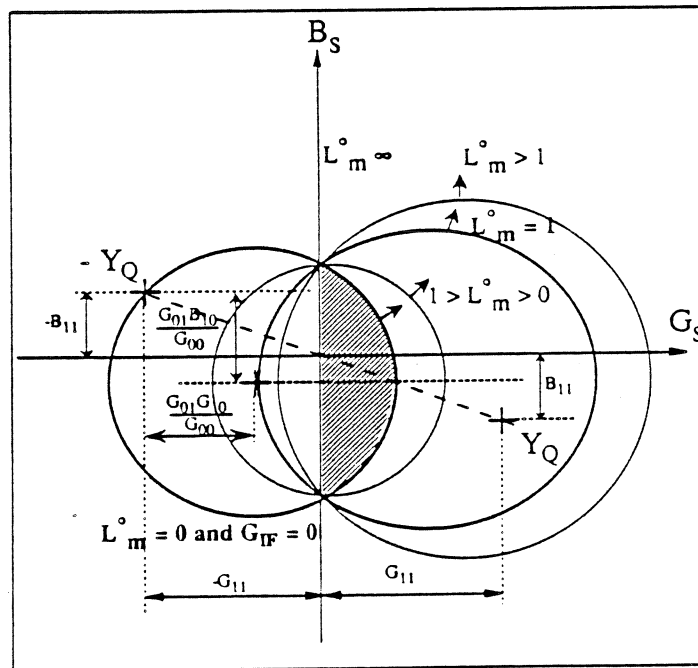


Figure 5: Contours of constant mixer available conversion gain. The hatched region corresponds to negative output conductance and infinite available gain. The centers of the circles are located on a line of constant susceptance and all circles cross two particular points on the  $G_S = 0$  axis.

One can notice that all these circles have their center on a line of constant susceptance equal to  $y_b$ . It is not the case for the circles of constant IF conductance whose centers are located on a line of slope  $B_{10}/G_{10}$ . This feature has been noticed in a particular case in [4]. It is in fact a very general behaviour of Double Side-Band mixers.

Also some contours of constant available conversion gain calculated by computer in [25] to be compared with experiments exhibit the same feature.

It is interesting to mention that this constant susceptance is the sum of two terms: the opposite of the quantum susceptance and  $(G_{10} B_{10})/G_{00}$ . On the other hand the mixer noise is minimized for source admittances close to the complex conjugate of the large-signal admittance which is also the quantum admittance [9, 26]. Since the receiver optimum performance is a trade-off between optimum mixer noise and optimum mixer gain, the susceptance for optimum receiver performance lies between  $B^*_Q$  with  $B_Q$  given by (2.10) and  $y_b$  where  $y_b$  is given by (4.5) as it can be seen in figure 5.

## V. OPTIMUM $\omega R_{NC}$ PRODUCT

The optimum  $\omega R_{NC}$  product is an important parameter of SIS junctions and it has been argued in Ref. [27] that it should vary as  $1/\omega$ . But this optimum value has been a controversial subject and it is argued in Ref. [26] that the choice of  $\omega R_{NC}$  product has to be made on technological grounds. One shows here that the optimum value is clearly dependent on the losses in the microwave environment of the junction. These losses can be due to the waveguide and backshort losses for waveguide mixers, dielectric losses for quasi-optical mixers but they are present also in the tuning circuits above the gap frequency of the superconductor, ...etc...

In any case the minimum normalized conductance which can be provided to the junction is  $1/R_{loss}$  if one calls  $R_{loss}$  the losses of the microwave environment normalized to the normal resistance of the junction  $R_N$ . In the source admittance plane  $(G_S, B_S)$  it means that the accessible environment admittances lie inside a circle of diameter  $1/R_{loss}$  centered on the  $B'_S = 0$  axis as is shown in figure 6.  $B'_S$  is the source admittance of the environment without the SIS junction capacitance  $C$  which has been included with the junction non-linear admittance. All admittances of figure 6 have been normalized to the normal conductance of the junction and, as a consequence, the  $\omega R_{NC}$  product is the distance between the  $B'_S = 0$  axis and the  $B_S = 0$  axis. This last axis was used for the construction of the contours of constant mixer IF conductance  $G_{IF}$  of figure 1 and constant available conversion gain of figure 5. They have been reproduced for clarity in figure 6. In this figure it appears that it is possible to get good performance if there is a common region between the disk of diameter  $1/R_{loss}$  and the admittances close to  $Y^*_Q$  where the mixer noise is minimum and close but outside the hatched region where the conversion gain is high. Then, if the losses are high, the accessible regions in the source admittance plane where it is possible to tune the mixer are inside a small circle which

may not intersect the regions of optimum performance. In that case, it is possible to overcome this problem by reducing the  $\omega R_N C$  product and, as a consequence, this product depends on the losses of the microwave environment. A mixer can achieve good performance with a high  $\omega R_N C$  product if the losses are low.

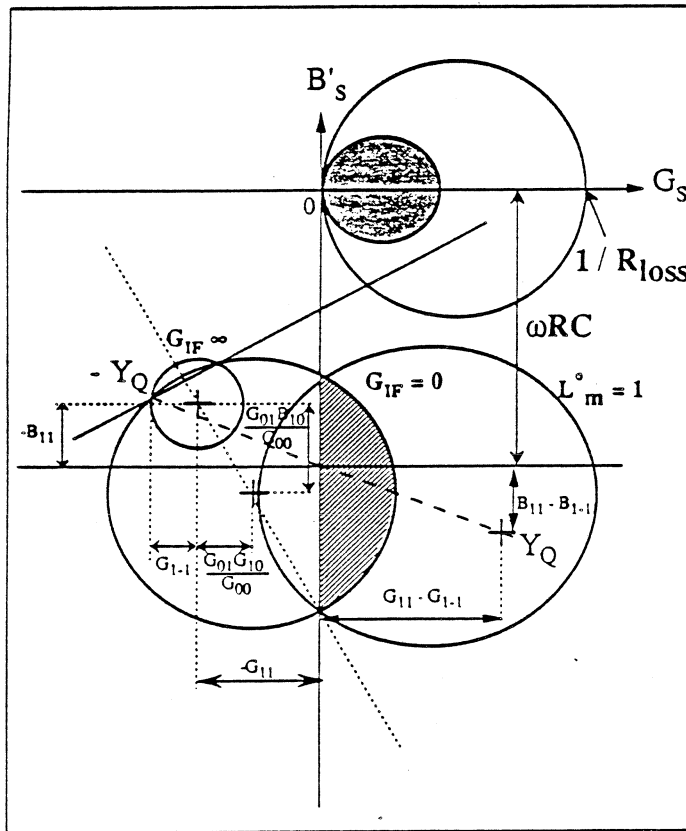


Figure 6: The accessible region in the source admittance plane which is limited by the microwave losses lies inside the circle of diameter  $1/R_{loss}$ . The junction capacitance has been included with the non-linear mixer admittance and the circles of constant available conversion gain and output admittance are translated by the  $\omega R_N C$  quantity. Good mixer performance can occur if the region inside the circle of diameter  $1/R_{loss}$  intersects the regions close to  $Y_Q^*$  and to the hatched region.

It is also possible to use this graphical formalism to understand an experimental fact which has been mentioned in particular in [21]. The region where the IF output differential conductance is negative (hatched region of figure 6) is associated to high conversion gain and consequently to high IF output power. But the source admittances for which such high gain occurs are far from the admittance  $Y_Q^*$  for minimum noise. As a result the receiver noise is high too. Then the receiver can be optimized for good



performance by providing source admittances closer to  $Y^*_Q$  and outside the hatched region of negative output conductance. It means that, in practice, the receiver must be optimized for maximum Y-factor and not for maximum IF power level. But if the losses or the mixer mount do not allow to reach the hatched region, then the maximum IF power levels roughly correspond to minimum noise then the technique which consists of maximizing the IF power is valid for most of cases when the slope of the I-V curve is positive.

## VI. CONCLUSION

Some graphical representations have been used to display in the source admittance plane the contours of constant IF output conductance and constant available gain of Double Side-Band mixers using the three-frequency approximation in the low IF limit. These contours have been determined analytically and are circles. Their properties are only dependent on the terms of the small-signal admittance matrix. This analysis applies to any mixer operated under the above assumptions, it has been used here for the case of SIS mixers. It is shown that this way of understanding the behaviour of a mixer allows to easily interpret many experimental facts like the influence of the quantum reactive terms with, in particular, the quantum susceptance or the  $\omega R_N C$  product. The two different modes of operation stated in Ref. [15] can also be easily visualized. Such an analytical tool is very useful to help the design of SIS mixers since it allows to determine analytically the regions in the source admittance plane for optimum mixer performance of a given DC I-V curve.

## ACKNOWLEDGEMENTS

The author wants to thank Gérard Beaudin and Pierre Encrenaz for continuing support. He also appreciated useful discussions with S.K. Pan, Qing Ke, M.J. Feldman, W.R. McGrath and M. Salez. The experimental I-V curve shown in this paper comes from an SIS junction fabricated by Sébastien George and Philippe Feautrier. This work has been performed at the DEMIRM of the Observatoire de Paris-Meudon - France.

## REFERENCES

- [1] J.R. Tucker, "Quantum limited detection in tunnel junction mixers," IEEE J. Quantum Electron., vol. QE-15, pp. 1234-1258, Nov. 1979.

- [2] J.R. Tucker and M.J. Feldman, "Quantum detection at millimeter wavelengths," *Rev. Mod. Phys.* **57**, pp. 1055-1113, Oct. 1985.
- [3] W.R. McGrath, P.L. Richards, A.D. Smith, H. van Kempen, and R.A. Batchelor, "Large gain, negative resistance, and oscillations in superconducting quasiparticle heterodyne mixers," *Appl. Phys. Lett.*, vol. 39, no. 8, pp. 655-658, Oct. 1981.
- [4] M.J. Feldman, S.K. Pan, A.R. Kerr, and A. Davidson, "SIS mixer analysis using a scale model," *IEEE Trans. Magnetics*, vol. MAG-29, pp. 494-497, May 1983.
- [5] C.A. Mears, Qing Hu, P.L. Richards, A.H. Worsham, D.E. Prober, and A.V. Räisänen, "Quantum limited quasiparticle mixers at 100 GHz," *IEEE Trans. Magnetics*, vol. MAG-27, pp. 3363-3369, March 1991.
- [6] S. Withington and E.L. Kollberg, "Spectral-Domain Analysis of Harmonic Effects in Superconducting Quasiparticle Mixers," *IEEE Trans. MTT*, vol. 37, no. 1, pp. 231-238, Jan. 1989.
- [7] C.E. Tong and R. Blundell, "Simulation of the Superconducting Quasiparticle Mixer Using a Five-Port Model," *IEEE Trans. MTT*, vol. 38, no. 10, pp. 1391-1398, Oct. 1990.
- [8] M.J. Feldman, "Theoretical considerations for THz SIS mixers," *Int. J. of Infrared and Millimeter Waves*, vol. 8, pp. 231-238, Jan. 1989.
- [9] D.P. Woody and M.J. Wengler, "Optimizing double-sideband SIS quasiparticle mixers," *IEEE Trans. Mag.*, vol. 27, pp. 3388-3390, March 1991.
- [10] C.E. Honingh, D. de Lange, M.M.T.M. Dierichs, H.H.A. Schaeffer, J. Wezelman, J. v.d. Kuur, Th. de Graauw and T.M. Klapwijk, "Comparison of Measured and Predicted Performance of a SIS Waveguide Mixer at 345 GHz," *Proceedings of the 3rd International Symposium on Space Terahertz Technology*, pp. 251-265, Ann Arbor, MI, March 24-26, 1992.
- [11] N.G. Ugras, A.H. Worsham, D. Winkler, D.E. Prober, "A superconducting Mixer Tuned by the Quantum Susceptance," *Proceedings of the 4th International Symposium on Space Terahertz Technology*, pp. 629-638, U.C.L.A., Los Angeles, CA, March 30-April 1, 1993.
- [12] T.M. Shen, "Conversion Gain in Millimeter Wave Quasi-Particle heterodyne Mixers," *IEEE J. Quantum Electron.*, vol. QE-17, pp. 1151-1165, July 1981.
- [13] M.J. Feldman, "Some analytical and intuitive results in the quantum theory of mixing," *J. Appl. Phys.*, vol. 53, no. 1, pp. 584-592, Jan. 1982.
- [14] M.J. Feldman, "An analytical investigation of the superconductor quasiparticle mixer in the low power limit," *IEEE Trans. Mag.*, vol. 27, no. 2, pp. 2646-2649, March 1991.
- [15] Q. Ke and M.J. Feldman, "Reflected power effects in computer simulations using the quantum theory of mixing," *IEEE MTT-S International Microwave Symposium Digest*, vol. 3, pp. 1425-1428, 1992 and Q. Ke and M.J. Feldman, "Signal and image port output power in the quantum theory of mixing," *this Symposium Proceedings*.

- [16] C.A. Mears, Q. Hu and P.L. Richards, "The effect of the quantum susceptance on the gain of superconducting quasiparticle mixers," *IEEE Trans. Mag.*, vol. 27, no. 2, pp. 3384-3387, March 1991.
- [17] Qing Hu, C.A. Mears and P.L. Richards, F.L. Lloyd, "Quantum susceptance and its effects on the high-frequency response of superconducting tunnel junctions," *Phys. Rev. B*, vol. 42, no. 16, pp. 10250-10263, December 1990.
- [18] J. Zmuidzinas and H.G. LeDuc, "Quasioptical slot antenna SIS mixers," *IEEE Trans. Microwave Theory Tech.*, vol. 40, no. 9, pp. 1797-1804, September 1992.
- [19] G. de Lange, C.E. Honingh, M.M.T.M. Dierichs, H.H.A. Schaeffer, H. Kuipers, R.A. Panhuyzen, T.M. Klapwijk, H. van de Stadt, M.W.M. de Graauw, E. Armandillo, "Quantum limited responsivity of a Nb/Al<sub>2</sub>O<sub>3</sub>/Nb SIS waveguide mixer at 460 GHz and first results at 750 and 840 GHz," *Proceedings of the 4th Int'l Symp. Space Terahertz Tech.*, pp. 41-49, U.C.L.A., Los Angeles, CA, March 30-April 1, 1993.
- [20] M. Salez, P. Febvre, W.R. McGrath, B. Bumble, H.G. LeDuc, "An SIS waveguide heterodyne receiver for 600 GHz to 636 GHz," *Int. J. of Infrared and Millimeter Waves*, vol. 15, no. 2, pp. 349-368, February 1994.
- [21] P. Febvre, W.R. McGrath, P. Batelaan, B. Bumble, H.G. LeDuc, S. George, P. Feautrier, "A low-noise SIS receiver measured from 480 GHz to 650 GHz using Nb junctions with integrated RF tuning circuits," to appear in: *Int. J. of Infrared and Millimeter Waves*, vol. 15, no. 6, June 1994.
- [22] S.K. Pan and A.R. Kerr, "A superconducting Tunnel Junction Receiver for Millimeter-Wave Astronomy," *NASA Technical Memorandum 87792*, pp. 52-67, 1986.
- [23] H.C. Torrey and C.A. Whitmer, *Crystal Rectifiers*. New-York: McGraw-Hill, 1948, M.I.T. Rad. Lab. Series, vol. 15.
- [24] M. Salez, P. Febvre, W.R. McGrath, B. Bumble, H.G. LeDuc, "High frequency effects and performance of a 600 GHz- 635 GHz SIS receiver using Nb/AlO<sub>x</sub>/Nb junctions," this symposium proceedings.
- [25] W.R. McGrath and P.L. Richards, D.W. Face and D.E. Prober, F.L. Lloyd, "Accurate experimental and theoretical comparisons between superconductor-insulator-superconductor mixers showing weak and strong quantum effects," *J. Appl. Phys.*, vol. 63, no. 8, pp. 2479-2491, April 1988.
- [26] Q. Ke and M.J. Feldman, "Optimum source conductance for high frequency superconducting quasiparticle receivers," *IEEE Trans. MTT.*, vol. MTT-41, pp. 600-605, April 1993.
- [27] A.R. Kerr and S.K. Pan, "Some recent developments in the design of SIS mixers," *Int. J. of Infrared and Millimeter Waves*, vol. 11, no. 10, pp. 1169-1187, October 1990.